Fragment Energy Correlation Measurements for ^{252}Cf Spontaneous Fission and ^{235}U Thermal-Neutron Fission*

H. W. Schmitt, J. H. Neiler,† and F. J. Walter‡

Oak Ridge National Laboratory, Oak Ridge, Tennessee

(Received 26 July 1965)

Fission-fragment mass and energy distributions and mass-versus-energy correlations have been obtained for ^{252}Cf spontaneous fission and ^{235}U thermal-neutron-induced fission. Silicon surface-barrier detectors were used in energy correlation measurements; absolute fragment energies were obtained by means of the mass-dependent energy calibration developed recently at this laboratory. Average total fragment kinetic energies before neutron emission are found to be 186.5±1.2 MeV for ^{252}Cf and 171.9±1.4 MeV for ^{235}U. Detailed experimental results are given and compared with those of other experiments. Observed fine structure in the fragment mass distribution and in the average total fragment kinetic energy as a function of mass is correlated with the energetically preferred even-even nucleon configurations in the fragments. New determinations of the root-mean-square width of the total-kinetic-energy distribution as a function of mass show structure which is also correlated with the energetically preferred even-even fragment configurations. Fission-neutron and gamma-ray data of other experiments are used with the new fragment kinetic energies presented here to examine the total energy balance for fission for the two cases studied.

I. INTRODUCTION

IN order to achieve an understanding of the fission process, it is essential that the details of the mass and energy distributions and mass-versus-energy correlations in fission at low excitation energies be known. It is desirable to obtain the absolute fragment energies as accurately as possible in order that valid, quantitative calculations of basic parameters, based on these energies and required to describe the fission process, may be made.

The development of solid-state detectors, with their inherent linear pulse-height response and generally good pulse-height resolution for charged particles, has permitted detailed investigations of fission fragment mass and energy distributions, mass-versus-energy correlations, and other fragment kinetic parameters associated with fission. The advantages of solid state detectors are evident: They may be made large (several square centimeters in area), thus allowing high counting efficiencies; the pulse-height-versus-energy response for a given ion mass is linear; and the resolution for heavy ions and fission fragments is reasonably good, i.e., $\lesssim 1.5$ MeV full width at half-maximum (FWHM).[1,2] The chief disadvantages are that the pulse-height response, while linear with energy, exhibits a pulse-height defect[3] which

is mass-dependent[1,2]; and that measurements are necessarily made of the fragment postneutron-emission energies, thus necessitating careful consideration of the effects of neutron emission in the determination of preneutron-emission quantities. The analysis of energy correlation experiments (more properly called pulse-height correlation experiments) is therefore a bit more complicated than might otherwise be the case; however, with the calibration method developed recently,[1,4] quite accurate quantitative determinations of the kinetic parameters and of the features of the various distributions are possible.

Historically, the postneutron-emission mass distributions in fission have been determined radiochemically and mass spectrometrically. A survey by Katcoff[5] gives results for thermal-neutron-induced fission (including those for ^{235}U); Nervik[6] has reported such determinations along with a summary of earlier results for ^{252}Cf spontaneous fission. More recently, the postneutron-emission mass distribution for ^{252}Cf spontaneous fission was determined at this laboratory from correlated energy and velocity measurements of single fragments.[4] Preneutron-emission mass and energy distributions and mass-energy correlations have in the past been deduced from double-ionization-chamber measurements[7]; more recently (also more precisely), they have been determined from double velocity measurements.[8-11] Two- and

* Research sponsored by the U. S. Atomic Energy Commission under contract with the Union Carbide Corporation.

† Present address: Oak Ridge Technical Enterprises Corporation (ORTEC), Oak Ridge, Tennessee.

‡ Present address: RIDL Division, Nuclear Chicago Corporation, Oak Ridge, Tennessee.

[1] H. W. Schmitt, W. M. Gibson, J. H. Neiler, F. J. Walter, and T. D. Thomas, Proceedings of the IAEA Conference on the Physics and Chemistry of Fission, Salzburg, Austria, 1965 (unpublished).

[2] C. W. Williams, W. E. Kiker, and H. W. Schmitt, Rev. Sci. Instr. **35**, 1116 (1964).

[3] Earlier studies of the pulse-height response of solid-state detectors to fission fragments include those reported by H. W. Schmitt, J. H. Neiler, F. J. Walter, and R. J. Silva, Bull. Am. Phys. Soc. **6**, 240 (1961); F. J. Walter, C. D. Moak, J. H. Neiler, H. W. Schmitt, W. M. Gibson, and T. D. Thomas, *ibid.* **8**, 39 (1963); H. C. Britt and H. E. Wegner, Rev. Sci. Instr. **34**, 274 (1963); and by F. J. Walter, IEEE Trans. Nucl. Sci.

NS-11, 32 (1964). A more recent report is that of E. Konecny and K. Hetwer, Nucl. Instr. Methods **36**, 61 (1965).

[4] H. W. Schmitt, W. E. Kiker, and C. W. Williams, Phys. Rev. **137**, B837 (1965).

[5] S. Katcoff, Nucleonics **18**, 201 (1960).

[6] W. E. Nervik, Phys. Rev. **119**, 1685 (1960).

[7] See, for example, D. C. Brunton and G. C. Hanna, Can. J. Res. **A28**, 190 (1950); D. C. Brunton and W. B. Thompson, *ibid.* **A28**, 498 (1950).

[8] S. L. Whetstone, Jr., Phys. Rev. **131**, 1232 (1963).

[9] J. S. Fraser, J. C. D. Milton, H. R. Bowman, and S. G. Thompson, Can. J. Phys. **41**, 2080 (1963).

[10] J. C. D. Milton and J. S. Fraser, Phys. Rev. Letters **7**, 67 (1961).

[11] J. C. D. Milton and J. S. Fraser, Can. J. Phys. **40**, 1626 (1962).
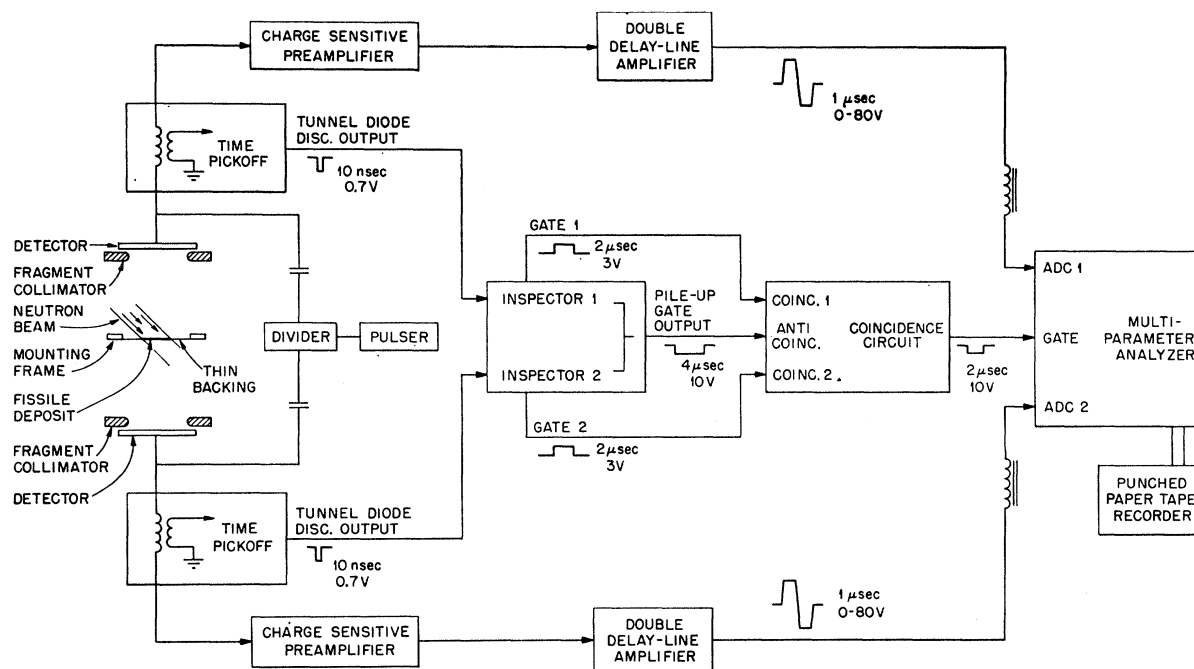
FIG. 1. Schematic diagram of source and detector arrangement and block diagram of electronic equipment
for fission fragment energy correlation experiments.

three-parameter energy correlation experiments with
solid-state detectors have been performed in recent
years for certain low-excitation fission cases,[12–14] al-
though complete results in at least the three cases cited
have not been reported because of the previous un-
certainties in absolute energy calibration of the data.

It will be our principal purpose in this paper to report
absolute values of fragment energies and other experi-
mental results, and to give quantitatively the features
of the mass and energy distributions and of the mass-
versus-energy correlations in the spontaneous fission of
^{252}Cf and in the thermal-neutron-induced fission of ^{235}U.
Some discussion of the total energy available for fission
is included; however, more complete interpretation of
the experimental results will be postponed until similar
experiments for other fissioning nuclei have been
analyzed.

II. METHOD AND APPARATUS

A schematic diagram of the experimental arrange-
ment and a block diagram of the instrumentation are
shown in Fig. 1. Although the method and arrangement
are self-explanatory, there are a few points which re-
quire special attention.

The fissile deposit and backing are both relatively
thin and uniform. The ^{252}Cf spontaneous fission source

was deposited by the self-transfer method (see ac-
knowledgments) onto a thin film of aluminum oxide in
which the energy loss for fission fragments was $\lesssim 4$ MeV,
as determined from a comparison of spectra obtained
with the deposit facing a detector and facing away from
the same detector. The source strength was $\sim 3 \times 10^5$
fissions per minute, and the ^{252}Cf deposit was about
1 cm^2 in area. The ^{235}U target was prepared by vacuum
evaporation of ^{235}UF$_4$ onto a carbon film about 20 μg/cm^2
thick, for which the fragment energy loss was $\lesssim 3$ MeV.
The deposit thickness was about 20 μg/cm^2, and the area
was about 1 cm^2. The purity of the sample was $>99\%$,
and a negligible fraction of the impurity content con-
sisted of other thermally fissionable material. The
neutron beam from the Oak Ridge Research Reactor
was collimated, so that no part of the beam struck the
target-mounting frame, detectors, or any other parts
inside the chamber.

The fragments were collimated with rounded, i.e.,
doughnut shaped, collimators. There are generally edge
effects associated with solid-state detectors; these may
occur at the edge of the silicon itself, where possible
lower electric fields may give rise to reduced pulse
heights, or at the inside edge of a protective layer
(usually epoxy), where some of the fragments may be
degraded in energy before entering the silicon. Use of a
collimator, as shown in Fig. 1, prevents detection of
fragments which might be subject to such effects. The
rounded, "doughnut-like" shape of the collimator mini-
mizes the number of degraded and accidentally scat-
tered fragments which are detected, provided the effec-

[12] W. M. Gibson, T. D. Thomas, and G. L. Miller, Phys. Rev.
Letters 7, 65 (1961).
[13] H. W. Schmitt, J. H. Neiler, F. J. Walter, and A. Chetham-
Strode, Phys. Rev. Letters 9, 427 (1962).
[14] F. J. Walter, H. W. Schmitt, and J. H. Neiler, Phys. Rev. 133,
B1500 (1964).

TABLE I. Notation.

*	Denotes quantities for preneutron-emission fragments
$\langle \rangle$ or bar	Denotes average quantities, as indicated
A	Mass of fissioning nucleus
a_i, a_i' b_i, b_i'	Constants in energy calibration Eq. (12)
B_{ni}	Binding energy of nth neutron emitted from ith fragment
B_{Ni}	Total binding energy associated with neutrons emitted from ith fragment
E_{ki}^*	Preneutron-emission kinetic energy of ith fragment
E_{ki}	Postneutron-emission kinetic energy of ith fragment
E_K^*	Total preneutron-emission fragment kinetic energy
E_K	Total postneutron-emission fragment kinetic energy
E_{Ri}	Center-of-mass recoil energy of neutron-emitting fragment
E_{xi}^*	Preneutron-emission excitation of ith fragment
E_{xT}^*	Total preneutron-emission fragment excitation energy
$E_{\gamma i}$	Gamma decay energy for ith fragment
$E_{\gamma T}$	Total fragment gamma decay energy
FWHM	Full width at half maximum
H	Subscript indicating heavy fragment
i	$i=1, 2$; subscript index indicating first or second fragment, corresponding to first or second detector
J	Jacobian, used in transformations of variables
L	Subscript indicating light fragment
m_i^*	Preneutron-emission mass of ith fragment; $m^*=$single fragment mass without regard to index i
m_i	Postneutron-emission mass of ith fragment; $m=$single fragment mass without regard to index i
N	Number of events or counts
Q	Total energy available for nuclear reaction (fission)
x_i	Channel number for ith fragment, corresponding to ith detector
Z, N	Proton, neutron number of nucleus
η_i	Average center-of-mass kinetic energy of neutrons emitted from ith fragment
μ_i	Provisional mass of ith fragment, defined by Eqs. (7) and (8)
ν_i	Number of neutrons emitted from ith fragment
ν_T	Total number of neutrons emitted from fragments
ξ_i	See Eq. (6)
σ	Root-mean-square width; square root of second central moment; the distribution variable is indicated in subscript

tive collimator surface area available to small-angle scattering[15] is kept as small as possible while maintaining a radius large enough to completely stop the fragments incident at larger angles. Accordingly, we have used $\frac{1}{16}$-in.-thick aluminum collimators, carefully rounded on the inside edges, with circular apertures of 3.5 to 3.8 cm² area—slightly smaller than the total effective detector area. In this arrangement, low-energy pulses due to tailing effects were almost completely absent. (These effects are not so important for light particles such as protons or alpha particles, and the problem of collimation is different in those cases.)

The detectors were surface barrier detectors, $\sim$4 cm² in area, matched as closely as possible. They were fabricated from $\sim$500-Ω-cm n-type silicon, and the front electrode of each detector consisted of a vacuum-evaporated gold film about 40 μg/cm² thick. The pulse-height response of these detectors was found to saturate satisfactorily (that is, the same pulse heights and peak-

to-valley ratios were obtained) for bias voltages between 50 and 200 V. A bias voltage of $\sim$100 V was maintained throughout the experiments. The detectors exhibited alpha-particle resolutions of $<$60 keV when tested with a standard low-noise, charge-sensitive amplifier.

Details of the electronic system used in the ^{235}U experiment are given in a previous publication.[16] The logic circuitry has been changed somewhat, and the present system, used in the ^{252}Cf experiment, is shown in Fig. 1. In both cases, circuits are included to minimize background and pile-up pulses, including "alpha-on-fission" events. Data were recorded event-by-event on punched paper tape; 128×128 channels were used in the ^{235}U experiments, and 256×256 channels were used in the ^{252}Cf experiments. Each of the experiments reported here contains $\sim$10^6 events, although a number of runs of comparable magnitude were made to check various experimental effects and to establish optimum conditions for the experiments.

III. ANALYSIS

It is first necessary to establish the relation between the initial and final energies of a fragment, with respect to neutron emission. For this purpose, we consider a single fragment of initial mass m_i^*, final mass m_i after emission of ν_i neutrons, and initial and final kinetic energies E_{ki}^* and E_{ki}, respectively. (We use the asterisk to refer to the excited, preneutron-emission fragments; the subscript i refers to the ith fragment, $i=1, 2$. A summary of the notation used throughout this paper is given in Table I.) The neutrons are assumed to be emitted after the fragment has been fully accelerated. The angular distribution of the neutrons in the fragment center-of-mass system is assumed to be isotropic. It is then easily shown that

$$\langle E_{ki} \rangle = (m_i/m_i^*)E_{ki}^* + E_{Ri}, \qquad (1)$$

where E_{Ri} is the center-of-mass recoil energy of the fragment. The energy E_{Ri} is of the order of 0.1 MeV or less and is negligible, for most purposes, compared with the first term of Eq. (1).

To analyze the energy correlation experiments, we assume that mass and linear momentum are conserved before neutron emission. That is,

$$m_1^* E_{k1}^* = m_2^* E_{k2}^*, \qquad (2)$$

$$m_1^* + m_2^* = A, \qquad (3)$$

where the subscripts refer to fragments 1 and 2 and where A is the mass of the fissioning nucleus. From the relation

$$m_i = m_i^* - \nu_i \quad (i=1, 2), \qquad (4)$$

it is easily shown that the mass m_1^* is related to the

[15] D. Engelkemeier and G. N. Walton, Report AERE-R 4716, 1964 (unpublished); also private communication, 1965.

[16] C. W. Williams, H. W. Schmitt, F. J. Walter, and J. H. Neiler, Nucl. Instr. Methods **29**, 205 (1964).

measured energies as follows (see also Ref. 17):

$$m_1^* = \frac{AE_{k2}}{E_{k2}+E_{k1}(1+\xi_1)}, \qquad (5)$$

where

$$\xi_1 = \frac{1+\nu_1/m_1}{1+\nu_2/m_2} - 1 \cong \nu_1/m_1 - \nu_2/m_2. \qquad (6)$$

The equations for m_2^* are obtained by interchanging subscripts.

In most energy correlation experiments, the values of ν_1 and ν_2 are not known as functions of both mass and energy, as would be required in Eqs. (5) and (6). Thus it appears most reasonable at present to analyze the energy correlation data according to simple, approximate relations, and then to correct the functions and distributions of interest as accurately as possible for effects of neutron emission.[18]

We write the following equations:

$$\mu_1 E_{k1} = \mu_2 E_{k2}, \qquad (7)$$

$$\mu_1 + \mu_2 = A, \qquad (8)$$

where now the μ_i are provisional fragment masses and are obtained from measured energies E_{k1} and E_{k2} as indicated in Eqs. (7) and (8). These quantities are not expected to differ greatly (<2 amu) from the correct masses m_i^*, inasmuch as both fragments emit neutrons and the error is to some extent cancelled by the use of E_{k1} and E_{k2} in Eq. (7). It is readily shown that m_1^* is related to μ_1 and μ_2 through the equation

$$m_1^* = \mu_1[1+\xi_1 E_{k1}/(E_{k1}+E_{k2})]^{-1}. \qquad (9)$$

Expressing μ_1 solely in terms of the m_1^* and ν_i, we have

$$\mu_1 = m_1^*(1+\xi_1)(1+\xi_1 m_1^*/A)^{-1}$$
$$\cong m_1^*(1+\xi_1 m_2^*/A). \qquad (10)$$

The energies of Eqs. (7) and (9) are obtained with the aid of the mass-dependent pulse-height-calibration equations for the particular detectors used in the experiment. It is sufficiently accurate, in most cases, to use the μ_i in the calibration equations, inasmuch as the coefficients of the mass-dependent terms are small enough so that errors in mass up to a few atomic mass units give rise to errors in energy of less than about 0.2 MeV.

Detailed total kinetic energy distributions as a function of fragment mass (or mass distributions as a function of total kinetic energy) are useful for study and comparison in formulating descriptions of the fission process. Thus we transform the data in the original pulse height versus pulse height matrix $N(x_1,x_2)$ to a

provisional mass versus total kinetic energy matrix $N(\mu_1,E_K)$ by means of the equation

$$N(\mu_1,E_K) = N(x_1,x_2)J\begin{pmatrix} x_1 & x_2 \\ \mu_1 & E_K \end{pmatrix}, \qquad (11)$$

where $E_K = E_{k1}+E_{k2}$, the total measured kinetic energy of the fragments. The mass-dependent energy calibration equations[1,4] are

$$E_{ki} = (a_i+a_i'\mu_i)x_i+b_i+b_i'\mu_i, \qquad (i=1,2), \qquad (12)$$

where we have used the provisional masses μ_i instead of the m_i. The appropriate equations for the transformation are then as follows:

$$x_1(\mu_1,E_K) = \frac{E_K(1-\mu_1/A)-b_1'\mu_1-b_1}{a_1+a_1'\mu_1}, \qquad (13)$$

$$x_2(\mu_1,E_K) = \frac{\mu_1 E_K/A-b_2'A+b_2'\mu_1-b_2}{a_2'A-a_2'\mu_1+a_2}, \qquad (14)$$

$$J\begin{pmatrix} x_1 & x_2 \\ \mu_1 & E_K \end{pmatrix} = \left| (a_1+a_1'\mu_1)^{-1}(a_2+a_2'A-a_2'\mu_1)^{-1} \right.$$
$$\times\left[\left(\frac{\mu_1}{A}\right)\left(\frac{a_1E_K/A+a_1b_1'+a_1'E_K-b_1a_1'}{a_1+a_1'\mu_1}\right) \right.$$
$$\left. \left. + \left(1-\frac{\mu_1}{A}\right)\left(\frac{a_2E_K/A+a_2b_2'+a_2'E_K-b_2a_2'}{a_2+a_2'A-a_2'\mu_1}\right) \right] \right|. \qquad (15)$$

Although the equations are cumbersome, they are straightforward and have been programmed for computer use. We note in Eq. (11) that the value of $N(x_1,x_2)$ is required at the point x_1,x_2 corresponding to the chosen values of μ_1,E_K. This quantity is obtained by a quadratic interpolation method described in a previous paper in connection with another experiment.[4]

An alternative to the transformation described in the preceding paragraph for obtaining the array $N(\mu_1,E_K)$ is as follows: The cells (1 channel$\times$1 channel) in the data array $N(x_1,x_2)$ are subdivided into a number of smaller subcells, and the number of counts in the original unit is divided equally among the subcells.[19] The coordinates μ_1,E_K are then calculated for the center of each of these subcells, and the assigned counts are then added to those in the μ_1,E_K interval in which the coordinates fall. We have analyzed the data of the present experiment by this method; each of the original units in the data array were divided into 100 subcells for this analysis. Although the results of the two methods are in generally good agreement throughout the arrays, we feel (1) that the interpolation method is somewhat better where the statistical uncertainties in the data are

[17] J. Terrell, Phys. Rev. 127, 880 (1962).

[18] In another approach, used, for example, in the ^{252}Cf fission fragment x-ray experiments of Glendenin et al. (Proceedings of the IAEA Conference on the Physics and Chemistry of Fission, Salzburg, Austria, 1965), the correction is made event by event in the analysis of the data, where the average value of $\nu(m^*)$ is used independent of the total fragment kinetic energy. The results are in agreement with those given here for ^{252}Cf.

[19] The subcell method has been discussed by J. C. D. Milton and J. S. Fraser in Ref. 11; comparisons of several methods of multi-parameter data analysis have been reported by T. D. Thomas and W. M. Gibson, Report NYO 10595, 1963 (unpublished).
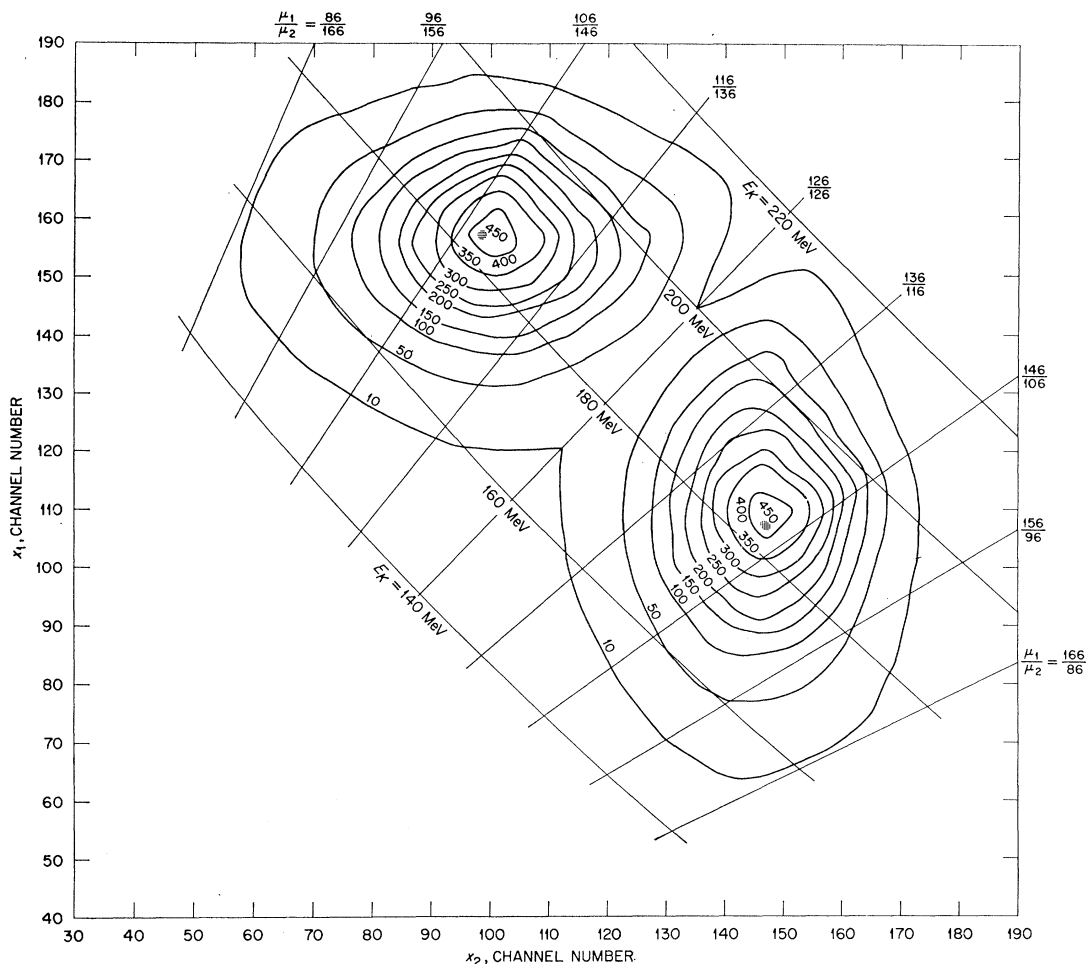
FIG. 2. Data array $N(x_1,x_2)$ for ^{252}Cf spontaneous fission. Numbers labeling the contours indicate the number of events per cell (1 channel $\times$1 channel). Curves of constant E_K and of constant μ_1/μ_2 are included. This array contains $\sim$0.83$\times$10^6 events.

small, so that advantage may be taken of the local shapes of the distributions, and (2) that the "sub-boxing" calculation is somewhat better in regions where the statistical uncertainties are large and the number of counts is small. The results presented in the next section have been taken from both analyses in accordance with this evaluation, although only slight differences would occur if either analysis were used alone.

From the array $N(\mu_1,E_K)$, we may now obtain the distribution of provisional masses, $N(\mu_1)$:

$$N(\mu_1) = \sum_{E_K} N(\mu_1,E_K). \qquad (16)$$

Then with a knowledge of the average number of neutrons emitted as a function of fragment mass, $\nu(m_1^*)$, we may obtain the preneutron-emission mass distribution $N(m_1^*)$ from the relation

$$N(m_1^*)dm_1^* = N(\mu_1)\left|\frac{d\mu_1}{dm_1^*}\right|dm_1^*, \qquad (17)$$

where in the present analysis the derivative is obtained numerically. $N(\mu_1)$ is determined (by interpolation) at

the value of μ_1 corresponding to a particular integral value of m_1^*.

Similarily, we obtain the average measured (post-neutron-emission) total fragment kinetic energy $\langle E_K \rangle$ as a function of μ_1 from the relation

$$\langle E_K(\mu_1) \rangle = \sum_{E_K} E_K N(\mu_1,E_K)/\sum_{E_K} N(\mu_1,E_K). \qquad (18)$$

Again, from a knowledge of $\nu(m_1^*)$ we determine the value of μ_1 corresponding to a particular m_1^* from Eq. (10); then we obtain the average initial, preneutron-emission, total kinetic energy $\langle E_K^*(m_1^*) \rangle$ from the equation

$$\langle E_K^*(m_1^*) \rangle = \langle E_K(\mu_1) \rangle \left(1 + \frac{\nu_1}{A}\frac{\mu_2}{m_1} + \frac{\nu_2}{A}\frac{\mu_1}{m_2} \right), \qquad (19)$$

where $E_K(\mu_1)$ is obtained for the values of μ_1 corresponding to the chosen value of m_1^*.

The energy resolution inherent in fragment energy correlation measurements is determined by the inherent resolution in the detectors and by the distributions in angle of emission, number, and energy of the neutrons
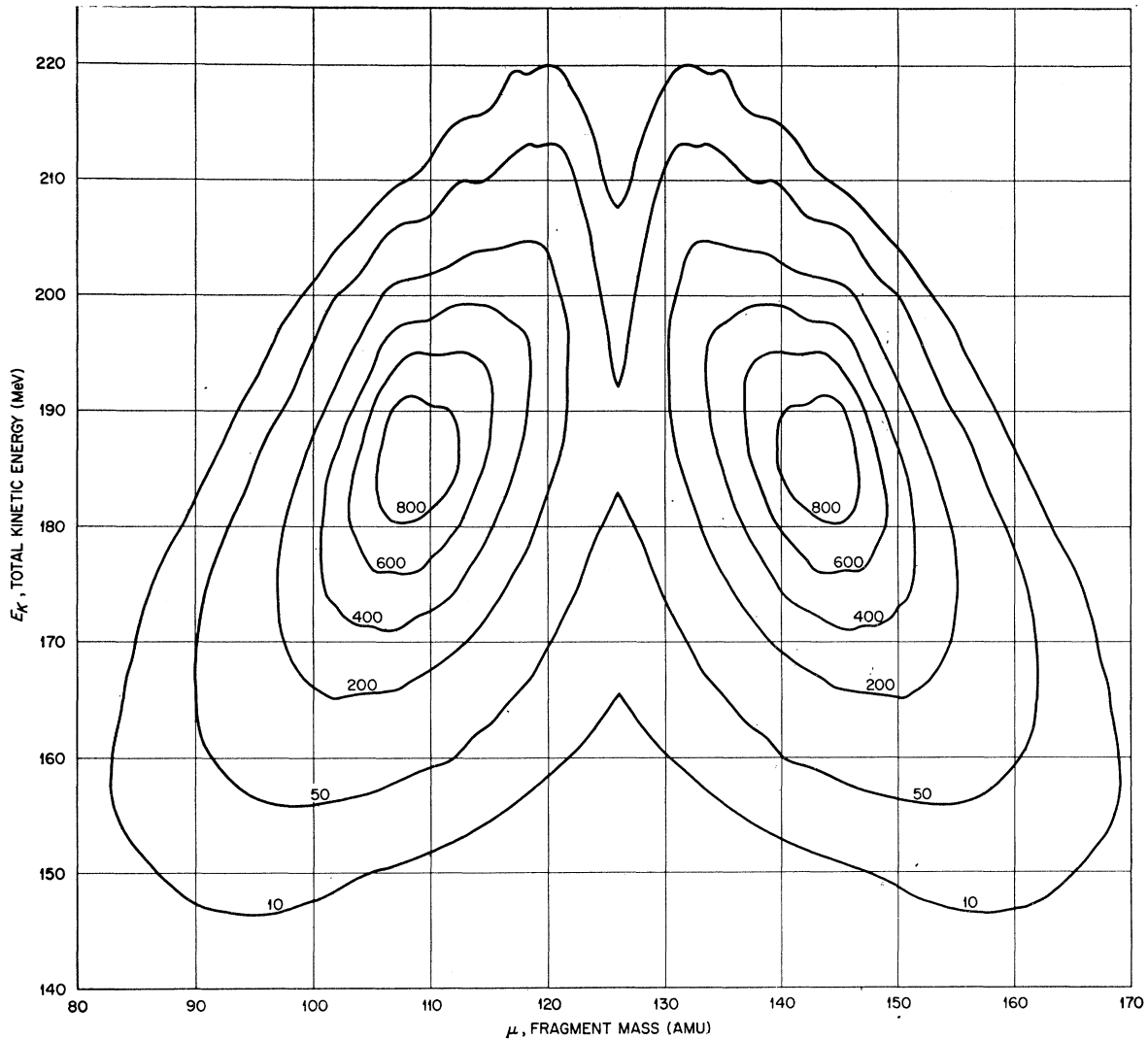
FIG. 3. Provisional mass versus total kinetic-energy array $N(\mu,E_K)$ for ^{252}Cf spontaneous fission.
Numbers labeling the contours indicate number of events per MeV per amu.

emitted. The detector resolution has been measured and is of the order of 1.5 MeV (FWHM).[1,2] The effects of neutron emission have been discussed by Terrell.[17] It may be shown that the total variance of the mass resolution function is approximated by

$$\sigma^2(m_1{}^*)=\frac{4\nu_T m_1{}^* m_2{}^* \eta}{3AE_K{}^*}+\tfrac{1}{4}\sigma^2(\nu_T)$$

$$+\frac{0.41}{E_K{}^{*2}}(m_1{}^{*2}+m_2{}^{*2}),\quad(20)$$

where $\nu_T=\nu_1+\nu_2$, η is the average center-of-mass energy of the neutrons, and $\sigma^2(\nu_T)$ is the variance of the distribution of ν_T. The first two terms approximate the variance in mass due to neutron effects, and the third

term takes into account the average energy resolution of the detectors.[20]

IV. RESULTS FOR ^{252}Cf SPONTANEOUS FISSION

The correlation data array $N(x_1,x_2)$ is shown in Fig. 2. Data were obtained in 256×256 channels, and a total of $\sim10^6$ events are included. The numbers labeling the contours indicate the number of events per cell (1 channel$\times$1 channel). Lines of constant total kinetic energy E_K and of constant provisional mass μ_1 or μ_2 are included. As indicated in the previous section, a transformation to the array $N(\mu_1,E_K)$ was carried out. This

[20] The expression given in Eq. (20) also appears in Ref. 18. The last term was somewhat reduced for those cases in the present work in which the average detector resolution width was less than 1.5 MeV, FWHM.
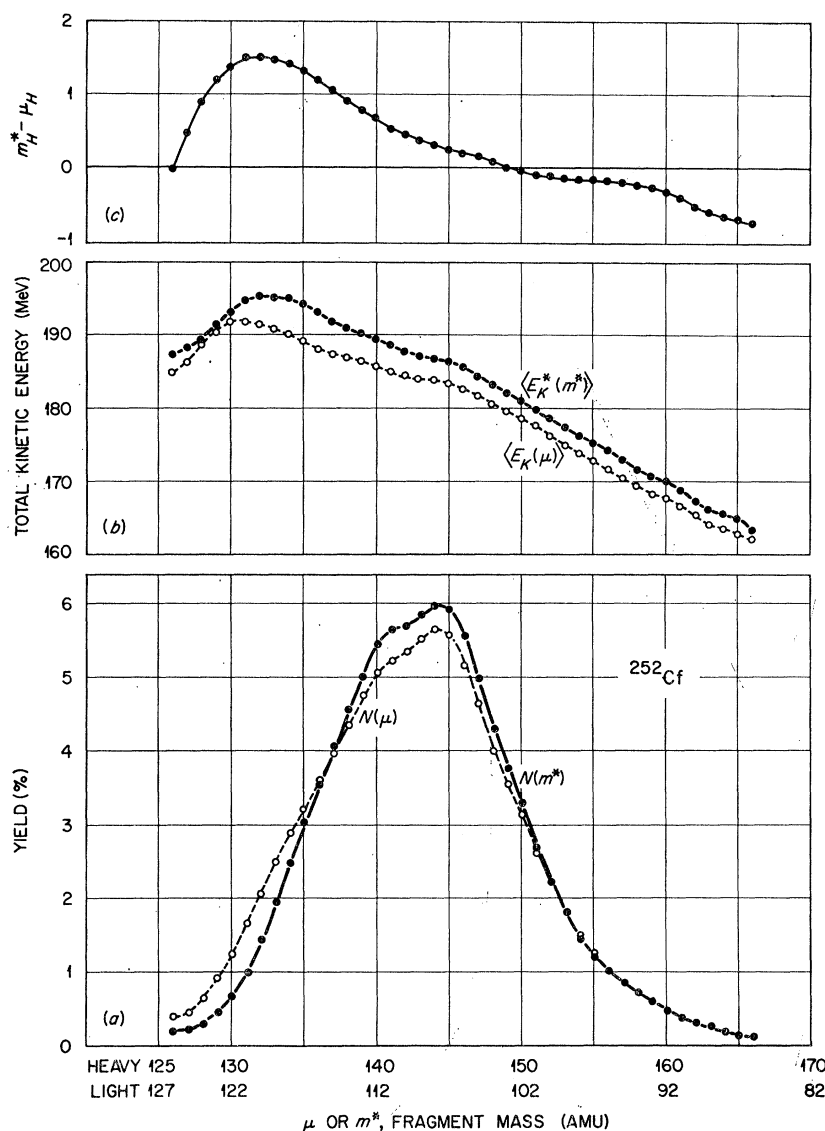
FIG. 4. Interim results for ^{252}Cf spontaneous fission. (a) Provisional-mass distribution $N(\mu)$ and pre-neutron-emission mass distribution $N(m^*)$. No corrections for resolution have been included. (b) $\langle E_K(\mu)\rangle$ and $\langle E_K{}^*(m^*)\rangle$. (c) $m_H{}^*-\mu_H$ versus $m_H{}^*$.

array is shown in Fig. 3; numbers labeling the contours indicate the number of events per MeV per amu.

Complete two-dimensional data giving ν as a function of fragment mass and kinetic energy would be required to construct lines of constant m_1^* or E_K^* in the above arrays or to construct the array $N(m_1^*,E_K^*)$. Such data have been obtained[21]; however, for general application to these and other energy correlation experiments we have taken the approach indicated in the previous section, that is, we derive the parameters and functions of interest from the $N(\mu_1,E_K)$ array and account for the effects of neutron emission in a separate step. The relation between μ_1 and m_1^*, based on the average neutron emission data of Bowman et al.,[21] is given in Fig. 4(c).

The fragment mass distribution obtained from the present experiment is shown in Fig. 4(a). For comparison, both the provisional mass distribution $N(\mu)$ and the preneutron-emission mass distribution $N(m^*)$ are shown; the latter is obtained from $N(\mu)$ and $\nu(m^*)$ as indicated in Sec. III. Similarly, the average total kinetic energy $\langle E_K(\mu)\rangle$, based on the provisional masses, is shown in Fig. 4(b) together with the total preneutron-emission kinetic energy $\langle E_K{}^*(m^*)\rangle$. The quantities $N(\mu)$ and $\langle E_K(\mu)\rangle$ are obtained directly from the present experiment together with the absolute energy calibration of Refs. 1 and 4. Thus they are independent of neutron-emission data and should provide a means for fairly direct comparison among energy correlation experiments.

In Fig. 5(a), we show the resolution-corrected pre-neutron-emission mass distribution for ^{252}Cf from the

[21] H. R. Bowman, J. C. D. Milton, S. G. Thompson, and W. J. Swiatecki, Phys. Rev. 126, 2120 (1962); 129, 2133 (1963).

TABLE II. Mean values and root-mean-square widths of the distributions.

Quantity	²⁵²Cf spontaneous fission			Postneutron-emission quant.	²³⁵U thermal-neutron fission	
	Preneutron-emission quantities				Preneutron-emission quantities	
	This work	Whetstone[a]	FMBT[b]	SKW[c]	This work	Milton & Fraser[d]
$\langle E_K^* \rangle$	186.5±1.2	185.7 ±1.8	182.1±1.7	...	171.9±1.4	167.68±1.7
$\sigma_{E_K}^*$	(12.0)[e]	11.3	15.2	...	(10.9)[e]	11.4
$\langle E_L^* \rangle$	106.2±0.7	105.71±1.06	104.4±1.0	103.77±0.5 (105.7)[f]	101.56	99.8 ±1.0
$\langle E_H^* \rangle$	80.3±0.5	80.0 ±0.8	78.3±0.7	79.37±0.5 (80.3)[f]	70.34	68.4 ±0.7
$\langle m_L^* \rangle$	108.55	108.4	107.8	106.0	96.57	95.93
$\langle m_H^* \rangle$	143.45	143.6	144.2	141.9	139.43	140.07
$\sigma_{m_L}^*$	6.72	6.77	7.27	6.53	5.36	5.829
$\sigma_{m_H}^*$	6.72	6.77	7.27	6.55	5.36	5.829

a Whetstone, Ref. 8.
b Fraser, Milton, Bowman, and Thompson, Ref. 9.
c Schmitt, Kiker, and Williams, Ref. 4.
d Milton and Fraser, Ref. 11.
e This is σ_{E_K} calculated from $N(\mu,E_K)$ and may not be exactly equal to $\sigma_{E_K}^*$.
f Preneutron-emission energies estimated from neutron corrections.

present experiment, compared with the resolution-corrected postneutron-emission mass distribution of the energy-velocity correlation experiment.[4] (The agreement of the latter distribution with the radiochemical mass distribution[6] has been cited in Ref. 4; see footnote 13 of Ref. 4 for method of resolution correction.) The differences in the two curves of Fig. 5(a) are readily understood in terms of the increase in $\nu(m^*)$ in each fragment group, as discussed previously.[4,9,17] The present preneutron-emission distribution is in good agreement with the resolution-corrected distribution of Whetstone.[8]

The average single-fragment preneutron-emission energy is shown as a function of fragment mass in Fig. 5(b); also the average total preneutron-emission kinetic energy is plotted as a function of fragment mass. The total kinetic energy curves of Whetstone[8] and Milton and Fraser[10] are shown for comparison. The agreement of the present results with those of Whetstone is well within the quoted uncertainties; the results of Fraser and Milton seem to disagree. This apparent discrepancy between the present results and those of the experiments of Fraser and Milton is now understood in terms of the effects of fragment scattering from the walls of the flight tubes in the double-velocity experiment.[22] These authors have, in fact, discussed the possible effects of scattering,[9] but the surprisingly large magnitude of the probability for fragment scattering at small angles to a surface was only recently found explicitly in the measurements of Engelkemeier.[15] Such scattering produces tailing toward lower velocities and energies, and thus somewhat broadens the derived mass distributions and alters the total kinetic energies, i.e., decreases them over most of the mass range. It should be noted, however, that the shape of the kinetic energy curve of Fraser and Milton

---

[22] Discussions with J. S. Fraser and J. C. D. Milton on this point are gratefully acknowledged. See also J. S. Fraser, Proceedings of the IAEA Conference on the Physics and Chemistry of Fission, Salzburg, Austria, 1965 (unpublished).
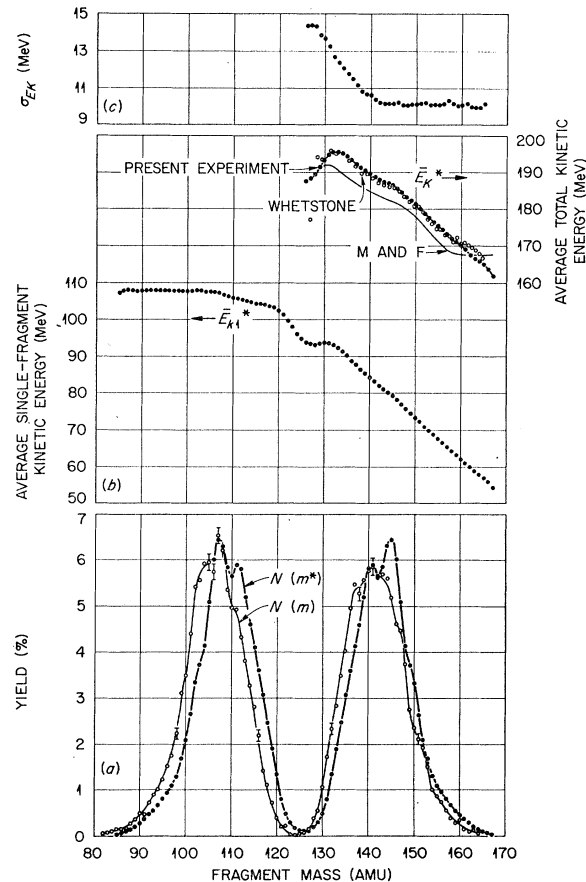

FIG. 5. Results for ²⁵²Cf. (a) Preneutron-emission mass distribution $N(m^*)$ corrected for resolution. The postneutron-emission mass distribution $N(m)$ is reproduced from Ref. 4. (b) Average single-fragment and total preneutron-emission kinetic energy as a function of mass. The total kinetic-energy curves of Whetstone (Ref. 8) and Milton and Fraser (Ref. 10) are shown for comparison; see text for discussion. (c) Root-mean-square width of total kinetic-energy distribution as function of fragment mass. Fine structure in the curves shown here is, in general, correlated with energetically preferred even-even fragment configurations.
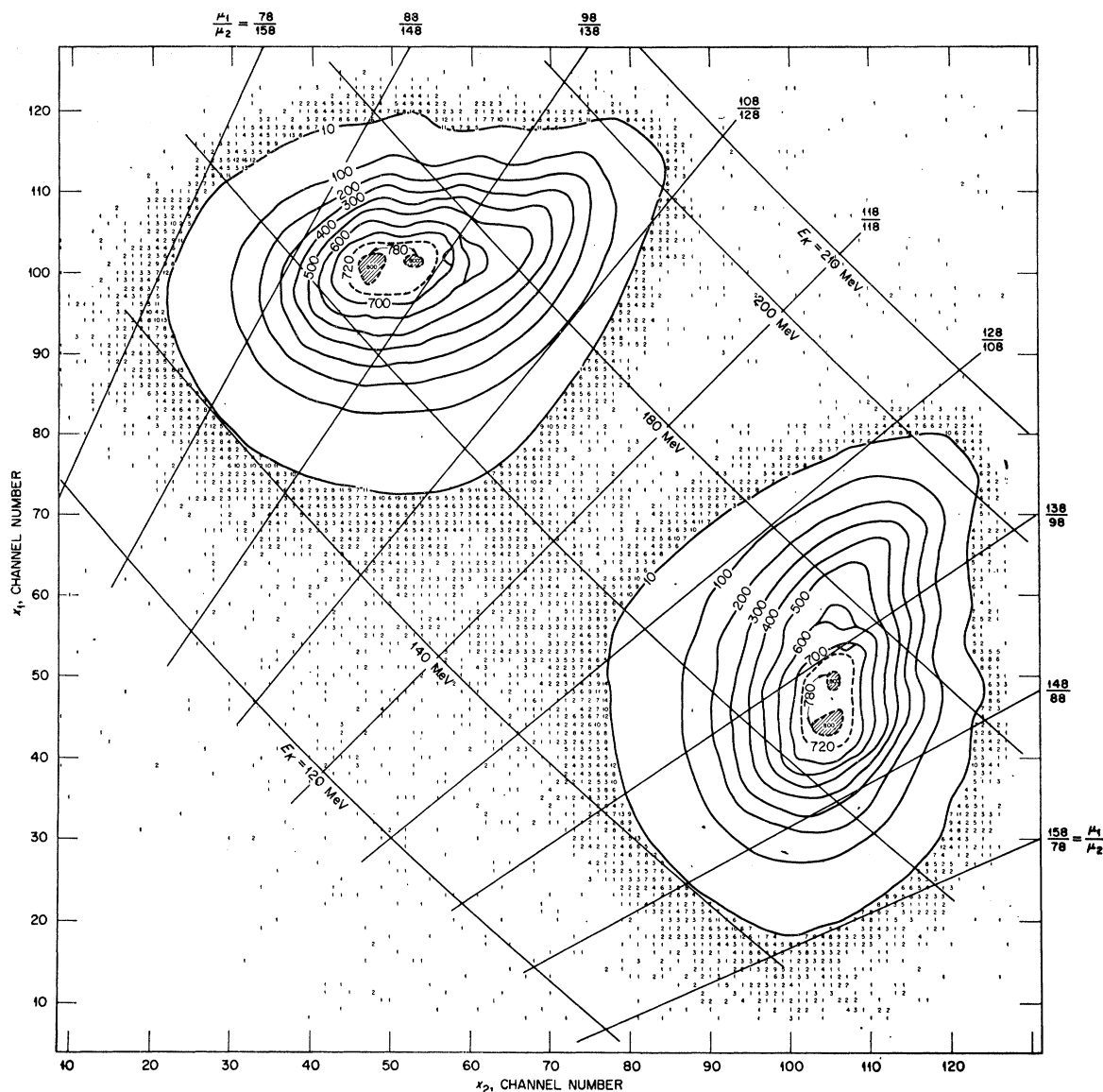
FIG. 6. Data array $N(x_1,x_2)$ for ^{235}U thermal-neutron-induced fission. Numbers labeling the contours and those appearing outside the 10-contours indicate the number of events per channel squared. Curves of constant E_K and of constant μ_1/μ_2 are included. This array contains $\sim 0.95 \times 10^6$ events.

for ^{252}Cf is similar to that of the present curve, and much of the structure is maintained; therefore the conclusions drawn by these authors[9–11] from the qualitative trends remain valid. The apparent absence of scattering effects in the curve of Whetstone is accounted for by the use of antiscattering baffles in that experiment.[8]

The rms width σ_{E_K} of the total kinetic energy distribution as a function of fragment mass is plotted in Fig. 5(c). The variation in ν as a function of total kinetic energy for a given mass division was neglected in computing this quantity. That is, the quantity $\sigma_{E_K}{}^2$, where

$$\sigma_{E_K}{}^2 \cong \langle E_K{}^2 \rangle - \langle E_K \rangle^2, \qquad (21)$$

was calculated as a function of μ, from the $N(\mu_1, E_K)$ array. The value of μ_1 corresponding to an integral value of $m_1{}^*$ was found, and $\sigma_{E_K}{}^2$ at this value was obtained by interpolation. It is the square root of this quantity which is plotted as a function of $m_1{}^*$ in Fig. 5(c).

A list of average fragment energies and masses and of some of the distribution widths is given in Table II. Detailed comparisons of these quantities with those of Whetstone show good agreement; comparisons of these quantities with the results of Milton and Fraser show discrepancies which are understood as discussed above. Only "direct computation" values are listed for comparison in the table; "Gaussian fit" values are included in the original papers, Refs. 8, 9, 11.
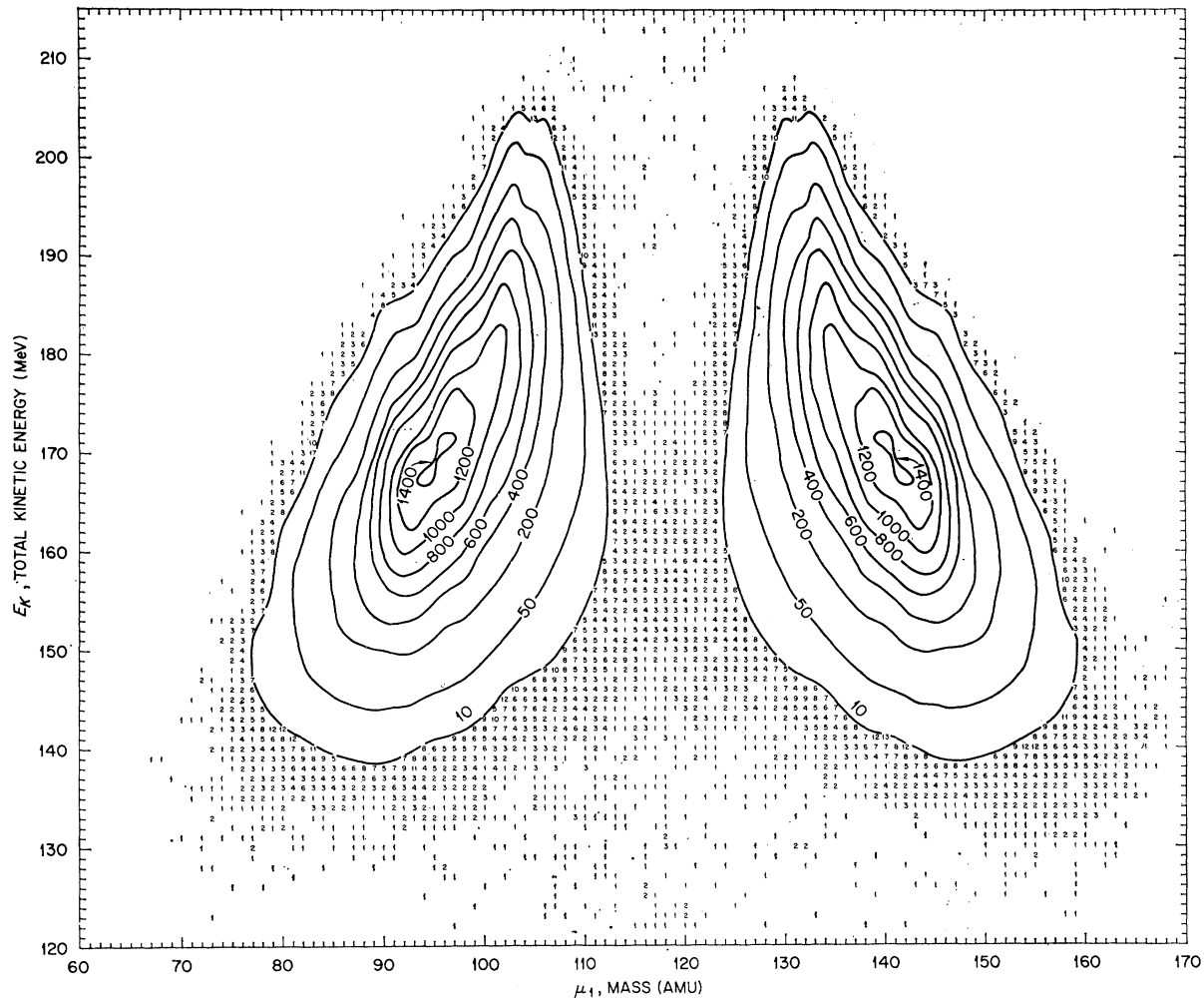
FIG. 7. Provisional mass versus total kinetic-energy array $N(\mu, E_K)$ for ^{235}U thermal-neutron-induced fission. Numbers labeling the contours and appearing outside the 10-contours indicate number of events per MeV per amu.

V. RESULTS FOR ^{235}U THERMAL-NEUTRON-INDUCED FISSION

The correlation data array $N(x_1, x_2)$ is shown in Fig. 6. Data were obtained in 128×128 channels and a total of $\sim 10^6$ events are included in this array. The numbers labeling the contours indicate the number of events per cell (1 channel $\times$ 1 channel), and lines of constant total kinetic energy E_K and of constant provisional mass μ_1, or μ_2, are included. Actual numbers of events have been entered outside the 10-contours in order to show the locations of rarer events.

In the case of ^{235}U, two auxiliary experiments were carried out. In the first, a ratio circuit and single-channel analyzer were incorporated in the system, so that only those events in a diagonal band running from lower left to upper right in Fig. 6 were recorded. The limitation in acquisition rate by the paper tape punch was thereby eliminated, and we were able to increase the number of recorded events in the symmetric region by a factor of

about four for the same time duration of the run, and thus to search with improved statistics for pileup and tailing effects.

In the second auxiliary experiment, a 32×32 channel analyzer was used to expand the region over a peak, so that a detailed examination of the contours at the peak was possible. These data were normalized to the pulse heights and numbers of events of the array shown in Fig. 6, and it is these results that show clearly the two separate peaks and the shapes of the contours indicated in the vicinity of the peaks. The results of these auxiliary experiments were incorporated in the final determinations of the mass-energy parameters and relationships discussed below.

Transformation of the $N(x_1, x_2)$ array to the $N(\mu_1, E_K)$ array yields the contour diagram shown in Fig. 7. The numbers labeling the contours and the numbers entered outside the last contours give the number of events per MeV per amu. The same treatment was carried out for
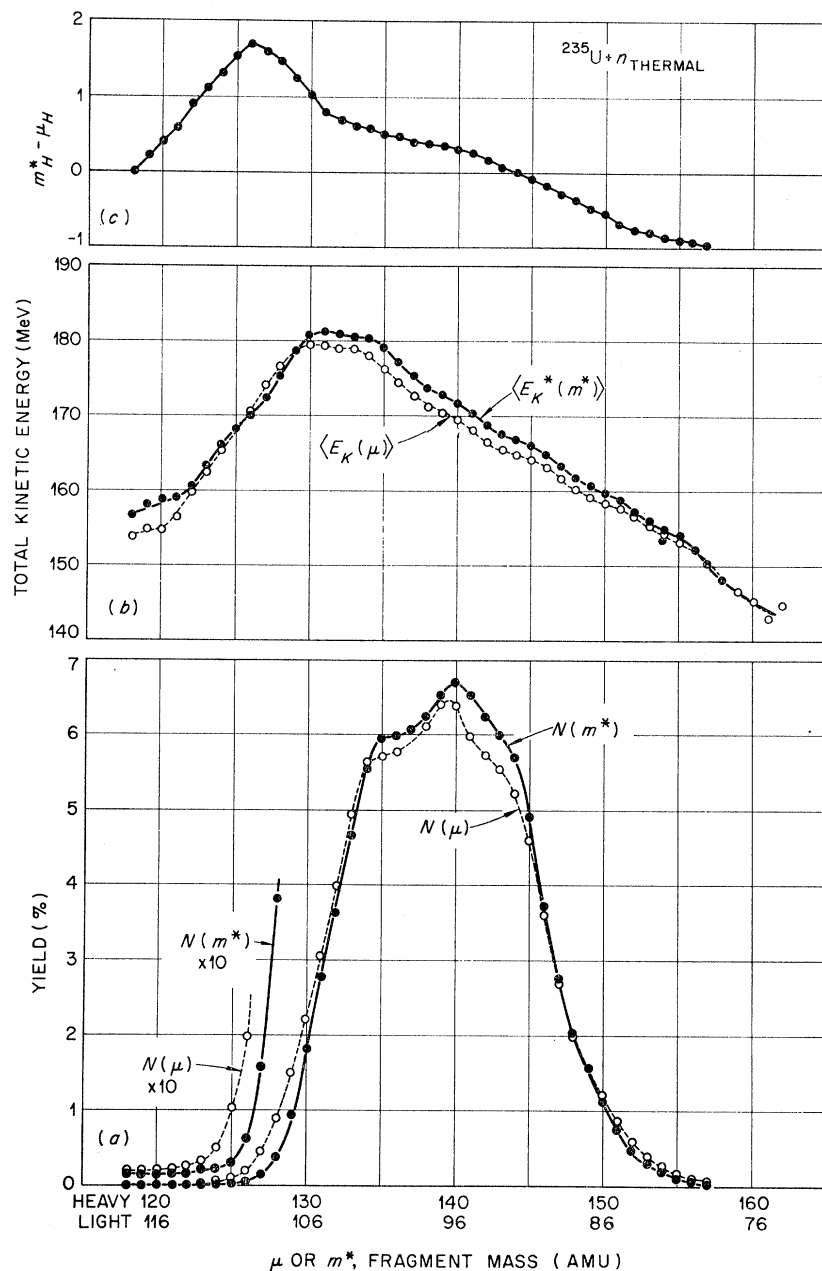
FIG. 8. Interim results for ^{235}U thermal-neutron fission. (a) Provisional mass distribution $N(\mu)$ and pre-neutron-emission mass distribution $N(m^*)$. No corrections for resolution have been included. (b) $\langle E_K(\mu) \rangle$ and $\langle E_K^*(m^*) \rangle$. (c) $m_H^* - \mu_H$ versus m_H^*.

these data as for the ^{252}Cf data; the neutron emission data of Apalin et al.[23] were used, and the relation between μ_1 and m_1^* is shown in Fig. 8(c).

As in the case of ^{252}Cf, we have plotted the provisional mass distribution $N(\mu)$ and the preneutron-emission mass distribution $N(m^*)$; these are shown in Fig. 8(a). In Fig. 8(b) are shown the quantities $\langle E_K(\mu) \rangle$ and $\langle E_K^*(m^*) \rangle$. The quantities $N(\mu)$ and $\langle E_K(\mu) \rangle$ are independent of the neutron emission data, as discussed above for ^{252}Cf.

[23] V. F. Apalin, Yu. N. Gritsyuk, I. E. Kutikov, V. I. Lebedev, and L. A. Mikaelyan, Nucl. Phys. 55, 249 (1964).

The mass-energy results for ^{235}U thermal-neutron fission are summarized in Fig. 9. The resolution-corrected preneutron-emission mass distribution from the present experiment is shown in Fig. 9(a) together with the radiochemical (postneutron-emission) mass distribution. The observed peak-to-valley ratio for the present distribution is about 450, compared to about 650 for the radiochemical distribution. The relationship between $N(m)$ and $N(m^*)$ is understood in terms of the increase in $\nu(m^*)$ in each fragment group, as discussed by Terrell.[17] The structure and features of the present preneutron-emission mass distribution are similar to

those of the distribution of Milton and Fraser,[11] although some differences, which are attributed to the scattering effects in the double-velocity experiment as discussed above, are observed. Further discussion of these mass distributions is included in Sec. VI.

The average single-fragment preneutron-emission kinetic energy as a function of fragment mass, $\langle E_{k1}^*(m^*)\rangle$ is shown in Fig. 9(b); also the average total preneutron-emission kinetic energy is plotted as a function of mass. The total kinetic energy curve of the double-velocity experiment of Milton and Fraser[10,11] is also shown. As discussed in Sec. IV for ^{252}Cf, the observed discrepancy is now understood in terms of the effects of fragment scattering in the double-velocity experiments; because of the small number of true events in the region of symmetry for ^{235}U, these effects are most severe in this region. Again note, however, that many of the conclusions drawn by these authors in connection with their double-velocity experiments,[10,11] e.g., with respect to structure, etc., remain valid.

The rms width σ_{E_K} of the total kinetic energy distribution as a function of fragment mass from the present experiment is plotted in Fig. 9(c). The method of calculation of this quantity is given in the last paragraph of Sec. IV.

Table II contains a list of average energies and masses and some of the widths of the distributions. In addition, the width of the single-fragment energy distribution for mass 97 fragments may be compared directly with a measurement by Cohen et al.[24] which involved radiochemistry and magnetic analysis. The observed value obtained in that work was 12.0±0.8% (FWHM), compared with 11.9% (FWHM) from the present work.

VI. DISCUSSION OF RESULTS

Discussion in this section will deal principally with total energy balance in the two fission cases studied and with a few general features of the results. As stated in the Introduction, the principal purpose of this paper is to present the experimental results; more detailed and quantitative interpretation of the results will be postponed until similar experiments for other isotopes have been analyzed.

A. Mass Distributions

It has been pointed out in a comparison[4] of the pre- and postneutron-emission mass distributions for ^{252}Cf that similar fine structure peaks appear in both distributions, with those in the postneutron-emission distribution appearing at slightly lower masses. Although Whetstone's preneutron-emission mass distribution[8] was used in that comparison, the same conclusion may be drawn from the comparison shown in Fig. 5(a). A further point of interest, however, is that the locations

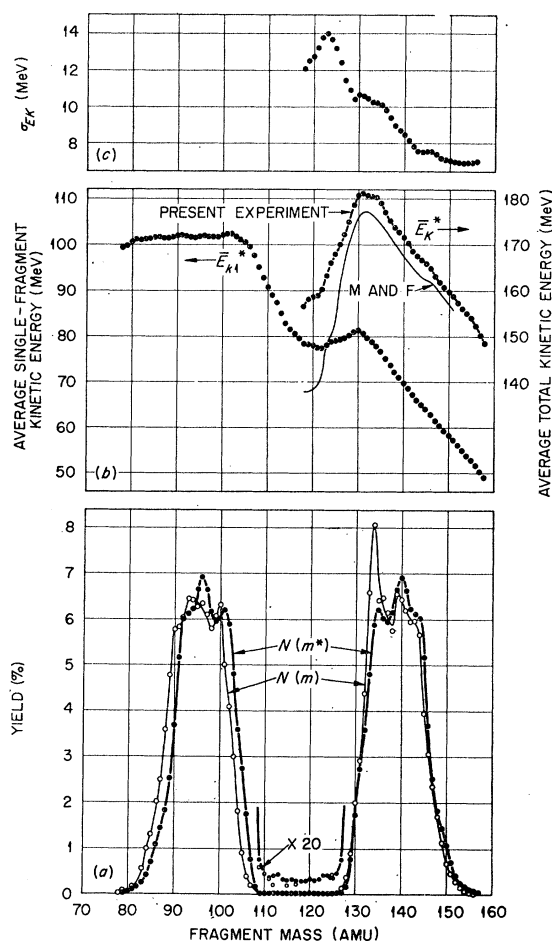[24] B. L. Cohen, A. F. Cohen, and C. D. Coley, Phys. Rev. 104, 1046 (1956).

FIG. 9. Results for ^{235}U thermal-neutron fission. (a) Preneutron-emission mass distribution $N(m^*)$ corrected for resolution. The postneutron-emission mass distribution $N(m)$ was obtained from Ref. 5. (b) Average single-fragment and total preneutron-emission kinetic energy as a function of mass. The total kinetic-energy curve of Milton and Fraser (Ref. 10) is shown for comparison; see text for discussion. (c) Root-mean-square width of total kinetic-energy distribution as a function of fragment mass. Fine structure in the curves shown here is, in general, correlated with energetically preferred even-even fragment configurations. Note that the maximum in $\sigma(m^*)$ occurs at $\sim$123 amu, where there are also fine-structure maxima in $N(m^*)$ and $\langle E_K^*(m^*)\rangle$.

(in mass) of some of the fine-structure peaks in the two distributions are nearly the same, especially in the regions of the peaks. This observation may reflect the higher binding energies of the nuclei corresponding to particular masses; the observed structure in ν as a function of mass[4,21,23] would also be a direct result of these relationships. Correlation of the fine-structure peaks in the primary mass distributions with the energetically preferred even-even configurations in the fragments, as suggested by Thomas and Vandenbosch,[25] is observed throughout the distributions, even in the valley of the ^{235}U distribution in the regions of $\sim$120 and $\sim$123 amu.

[25] T. D. Thomas and R. Vandenbosch, Phys. Rev. 133, B976 (1964).

We have carried out cumulative yield calculations[19],[26] to determine $\nu(m^*)$ from the pairs of mass distributions shown in Figs. 5(a) and 9(a). In both cases the resulting total number of neutrons $\nu_T(m^*)$ is essentially in agreement with measurements.[21],[23] In the case of ^{252}Cf, the calculated number of neutrons emitted from the light fragment is slightly larger than the measured[21] number; in the heavy fragment group the calculated number is slightly smaller than the measured number. Small experimental effects, unimportant in the other results of this experiment, could give rise to the observed differences. In the case of ^{235}U, however, the cumulative yield calculations indicate a definitely larger number of neutrons emitted from light fragment masses in the range ~90 to ~105 amu than the results of Apalin et al.[23] show. The cumulative yield results give a correspondingly smaller number of neutrons than the results of Apalin et al. for the complementary heavy fragments from ~130 to ~145 amu. Detailed consideration of experimental effects, such as low-energy tailing and various resolution effects in the present experiment, indicates that these are not large enough to be probable causes of the discrepancy. To discuss this result further, therefore, will require re-evaluation of excitation energies of individual fragments and other considerations which we shall postpone until the data of similar experiments for other isotopes are evaluated.

B. Kinetic Energies

The principal new results of the present experiments, with respect to the fragment kinetic energies, are the absolute values of the energies (which are higher than some of those of previous experiments) and the reduced dip in energy at symmetry. The experimental reasons for the observed discrepancies with other experiments are discussed in Secs. IV and V above. The present dip in average total kinetic energy, defined as the difference between the maximum value and the value at symmetry, is 8 MeV for ^{252}Cf and 24 MeV for ^{235}U.[27] In the case of ^{252}Cf, the narrow mass valley combined with resolution effects may render the absolute value of the dip somewhat more uncertain than in the case of ^{235}U.

The general features and qualitative interpretations of the kinetic energies as functions of fragment mass have been discussed many times in the literature; the same general features are observed again here. These features include (1) the maximum in average total kinetic energy for those fragments of mass 132–134 amu, in which the proton shell $Z=50$ is closed and/or the neutron shell $N=82$ is closed; (2) the dip in $\bar{E}_K^*$ at symmetry, which is thought to correspond to greater

deformability of both fragment nuclei in the region of symmetry; and (3) the near constancy of the average single-fragment kinetic energy as a function of mass throughout the light-fragment group, caused by almost exact compensation of (a) the decreasing total kinetic energy with decreasing light-fragment mass and (b) increasing fraction of total kinetic energy imparted to the light fragment, with decreasing light-fragment mass [cf. Eqs. (2) and (3)]. All of these features are present in both the ^{252}Cf and ^{235}U results.

The observed fine structure in the average total kinetic energy has been correlated with the energetically preferred even-even configurations in the fragments.[25] This correlation is observed in the present results; further discussion on this point is contained in C below.

C. Total Energy Balance

Probably more experimental data concerning the radiations from ^{252}Cf spontaneous fission and ^{235}U thermal-neutron-induced fission are available than are available for any other fission cases. Therefore, it is attractive to attempt to combine some of this information to obtain a total energy balance for each of these two cases.

The total energy available for fission into a given mass pair m_1^*, m_2^* (i.e., the Q value, defined as is usual for nuclear reactions) appears as kinetic and excitation energy of the fragments

$$Q = E_K^* + E_{x1}^* + E_{x2}^*, \qquad (22)$$

where the E_{xi}^* represent the excitation energies of the primary, i.e., preneutron-emission fragments. The excitation energy E_{xi}^* appears, in turn, in the form of neutrons and gamma rays:

$$E_{xi}^* = \sum_{n=1}^{\nu} B_{ni} + \nu_i \eta_i + E_{\gamma i}, \qquad (i=1, 2), \qquad (23)$$

where B_{ni} is the binding energy of the nth neutron emitted from the ith fragment, η_i is the average center-of-mass kinetic energy of neutrons from the ith fragment, and $E_{\gamma i}$ is the energy of prompt gamma rays emitted from the ith fragment.

For ^{252}Cf spontaneous fission, the average number of neutrons as a function of primary fragment mass, $\nu(m^*)$, and the average kinetic energy of the neutrons, $\eta(m^*)$, have been measured by Bowman et al.[21] The B_{ni} are readily obtained from semiempirical mass formulas (or tables); thus for a given fragment the total excitation energy appearing in the form of neutrons is given by the sum of the first two terms of Eq. (23). The total excitation energy E_{xT}^* for both fragments is given by $E_{x1}^* + E_{x2}^*$, or from Eq. (23):

$$E_{xT}^* = B_{N1} + B_{N2} + \nu_1 \eta_1 + \nu_2 \eta_2 + E_{\gamma T}, \qquad (24)$$

where we have designated the sums of the binding energies as B_{N1} and B_{N2} and where $E_{\gamma T} = E_{\gamma 1} + E_{\gamma 2}$.

[26] H. C. Britt and S. L. Whetstone, Phys. Rev. **133**, B603 (1964).

[27] This result for ^{235}U is in agreement with a recent result of N. K. Aras, M. P. Menon, and G. E. Gordon [Nucl. Phys. **69**, 337 (1965)] based on range measurements. A result has recently been reported also by T. D. Thomas, W. M. Gibson, and G. Safford, Proceedings of the IAEA Symposium on the Physics and Chemistry of Fission, Salzburg, Austria, 1965 (unpublished).

Thus the sum of the first two terms gives that part of the total excitation energy which appears in the form of neutron binding and is dependent on the particular mass formula employed. The sum of the first four terms is the total part of $E_{xT}*$ which appears in the form of neutrons, and $E_{\gamma T}$ is that part which appears as gamma rays.

In Fig. 10 we have plotted the average total kinetic energy and certain portions of the total excitation energy as functions of fragment mass for ^{252}Cf spontaneous fission. The curve labeled "neutron binding only" is based on the neutron measurements of Bowman et al.[21] and on neutron binding energies obtained from the Wing-Fong mass formula[28]; this curve corresponds to the sum of the first two terms of Eq. (24). The curve labeled "neutrons" corresponds to the sum of the first four terms of Eq. (24), where we have used the data of Bowman et al. for the neutron kinetic energy terms. The curve labeled "gammas" corresponds to the last term of Eq. (24) and is estimated to be approximately one-half of the binding energy of the first neutron not emitted; that is, if $\nu = 2.0$ for fragment 1, the quantity $E_{\gamma 1}$ is
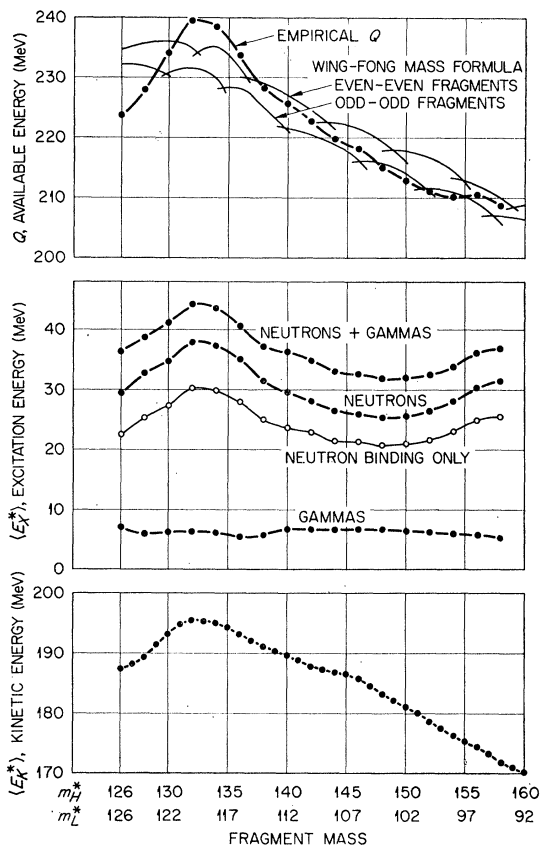
FIG. 10. Total energy balance for ^{252}Cf spontaneous fission. See text.

[28] J. Wing and P. Fong, Phys. Rev. **136**, B923 (1964); see also Argonne National Laboratory Report ANL-6886, 1964 (unpublished).
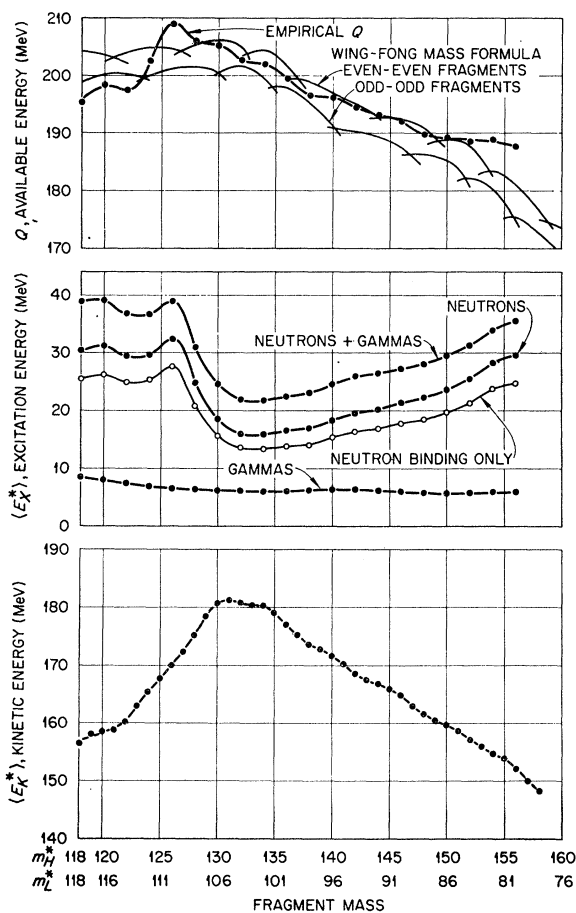
FIG. 11. Total energy balance for ^{235}U thermal-neutron fission. See text.

estimated to be one-half of the binding energy of the third neutron, and similarly for fragment 2. Since ν is, in general, not an integral value, suitable weighted averages are computed. The curve labeled "neutrons +gammas" is $E_{xT}*$ and is just the sum indicated. In the uppermost part of the figure we have plotted the "empirical Q," obtained as the sum of the experimental total kinetic and excitation energies. For comparison, the Q values calculated from the Wing-Fong mass formula for fission into even A nuclei are plotted; the upper parabolas are obtained for even-Z, even-N fragments, the lower parabolas for odd-Z, odd-N fragments. The Q values for fission into odd-A nuclei form a set of parabolas at energies between the two sets shown. We shall discuss the upper portion of Fig. 10 below along with the results for ^{235}U.

Calculations similar to those outlined for ^{252}Cf have been carried out for the thermal-neutron-induced fission of ^{235}U. The results are shown in Fig. 11. In this case, the values of $\nu(m*)$ were obtained from the measurements of Apalin et al.[23] and the neutron kinetic energy η was taken to be 1.2 MeV throughout. The gamma-ray

curve was obtained from the measurements of Maier-Leibnitz et al.[29] Again the Wing-Fong mass formula was used to obtain the neutron binding energies and the Q values shown as parabolas in the upper part of the figure.

The comparisons shown in the upper parts of Figs. 10 and 11 exhibit some interesting features. In particular, the agreement for ^{235}U between the empirical and calculated Q values over most of the mass range is quite good; the disagreement near symmetry may arise from two sources, namely, (1) the severe difficulties encountered in obtaining reliable experimental quantities near symmetry, and (2) the difficulty in accounting accurately for shell effects in a nuclear mass formula. In the case of ^{252}Cf, the same kind of discrepancy appears near symmetry, and the agreement is not as good over the rest of the mass range. It is known, however, that calculations based on extrapolations of a semiempirical mass formula to regions far from the stable mass valley should be considered quite uncertain.[30]

We have carried out similar calculations for ^{252}Cf and ^{235}U based on the mass formulas of Seeger[31] and Cameron.[32] In both these cases, the trends are similar to those shown here, and the locations of the even-even parabolas are in general the same for all three mass formulas. None of these mass formulas, however, predicts decreases in Q as large as appear at symmetry in the "empirical Q" curves of Figs. 10 and 11.

The fine-structure peaks which are observed in the average total kinetic energy are reflected in the empirical Q curve and are seen to agree in location with the even-even parabolas. This correlation was first suggested by Thomas and Vandenbosch[25] and indicates the influence of the energetically preferred even-even configurations in the fragments. The fine structure observed in the primary mass distributions are seen to be similarly correlated in location with the even-even parabolas, as also suggested by Thomas and Vandenbosch. The present observations are the first to our knowledge which indicate that structure in the width of the total kinetic energy distribution as a function of fragment mass [Figs. 5(c) and 9(c)] is also correlated with the even-even fragment configurations.

ACKNOWLEDGMENTS

[29] H. Maier-Leibnitz, H. W. Schmitt, and P. Armbruster, Proceedings of the IAEA Conference on the Physics and Chemistry of Fission, Salzburg, Austria, 1965 (unpublished).

[30] Discussions with P. Fong on this point are gratefully acknowledged.

[31] P. A. Seeger, Nucl. Phys. 25, 1 (1961). Q values for fission based on this mass formula have been tabulated by J. C. D. Milton, Report UCRL-9883 revised 1962 (unpublished).

[32] A. G. W. Cameron, Can. J. Phys. 35, 1021 (1957); also Chalk River Report CRP-690, 1957 (unpublished). Q values for fission based on this formula have been tabulated by J. C. D. Milton (see note, Ref. 28).